Modelling and simulation of CO2 bottoming cycles for offshore oil and gas installations at design and off-design conditions

Harald Taxt Walnum[a]*, Petter Nekså[a], Lars Olof Nord[b], Trond Andresen[a]

[a] SINTEF Energy Research,
NO-7465 Trondheim, Norway
Postboks 4761 Sluppen,
N-7465 Trondheim, Norway

[b] Norwegian University of Science and Technology,
Department of Energy and Process Engineering,
Kolbjørn Hejes v 1B
Trondheim 7491, Norway

* Corresponding author.
E-mail address: Harald.Taxt.Walnum@sintef.no,
Phone: +47 73597194,
Fax: +47 73593950,
Postal address: SINTEF Energy Research,
Postboks 4761 Sluppen,
N-7465 Trondheim, Norway

This is the accepted version of an article published in Energy
http://dx.doi.org/10.1016/j.energy.2013.06.071

Abstract

Improved energy efficiency is an issue of increasing importance in offshore oil and gas installations. The power on offshore installations is generated by gas turbines operating in a simple cycle. There is an obvious possibility for heat recovery for further power generation from the exhaust heat. However, the limited space and weight available makes the inclusion of bottoming cycles challenging. Due to its high working pressure and thereby compact components CO2 could be a viable solution, combining compactness and efficiency. An in-house simulation tool is used to evaluate the performance of CO2 bottoming cycles at design and off-design conditions. Both a simple recuperated single stage cycle and a more advanced dual stage system are modelled. Results from simulations show a potential for 10-11 %-points increase in net plant efficiency at 100 % gas turbine load. Also off-design simulations taking the variation in heat exchanger performance into account are performed showing that the bottoming cycle improves the off-design performance compared to the standard Gas Turbine solution. Even at 60 % GT load, the combined cycle with CO_2 bottoming cycle can achieve up to 45 % net plant efficiency, compared to 31 % for only the gas turbine.

Key words: Offshore, bottoming cycle, CO_2 power cycle, off-design, modelling and simulation

1 Introduction

Improved energy efficiency is an issue of increasing importance in offshore applications. One reason is the increasing awareness of global warming, which makes it generally desirable to reduce the CO_2 emissions per unit of produced oil or natural gas. This has led to the introduction of an offshore CO_2 tax in Norway.

Another reason is the declining production profile over time from any oil or gas field. Offshore facilities are normally designed for maximum production or “plateau” rates [1]. The rough picture, with many possible individual exceptions, is that after the plateau rate production phase is over, production of oil and gas will continue for many years at a declining rate, typically with increasing energy penalty, i.e., more energy is consumed per unit of oil or gas produced. This will increase the production cost, in addition to increasing the CO_2 emissions per unit of produced oil or gas. Improved energy efficiency will thus increase in importance during the lifetime of the field.

The offshore electric power is generated by gas turbines operating in a simple cycle. The hot exhaust gas from these gas turbines is emitted to the atmosphere, either directly or after recovering part of the exhaust heat for process purposes. Nguyen et al. [2] did an exergy analysis for a generic oil and gas platform located in the North Sea, showing that the gas turbine exhaust represents about 60 % of the exergy losses. There is an obvious possibility for heat recovery for further power generation from the exhaust heat. Already a few offshore installations have steam bottoming cycles implemented to increase the efficiency of the electricity production on the oil platform.

For onshore power production plants, the multi pressure level steam bottoming cycle is considered state of the art, with combined cycle efficiencies up to 60 %. However, this technology is rather voluminous and heavy and therefore not necessarily the best option for offshore applications. More compact steam cycles (single-pressure) has however been installed at the Norwegian Continental Shelf (NCS) [3]. More compact solutions with once-through steam generators (OTSG) have also been studied in order to improve this further. Nord and Bolland [4] describes challenges related to steam bottoming cycles offshore, and the potential for weight savings with OTSG compared to drum based systems, and further describes simulation results for design and off-design conditions for offshore OTSG combined cycles [5].

Lately, supercritical CO_2 Brayton cycles have received much attention, especially for nuclear applications. Johnson et al. [6] describes the development of CO_2 Brayton cycles for large scale

This is the accepted version of an article published in Energy
http://dx.doi.org/10.1016/j.energy.2013.06.071

nuclear, solar or fossil fuel power plants, Kimball and Clementoni [7] describes the development of a 100 kWe test loop focusing on component and control system development, and Wright et al. [8] describes experience with a laboratory test rig, challenges with scaling of the system and potential applications. The main reason for this increased interest is the potential for weight, size and cost reduction. These characteristics are also transferable to bottoming cycles for gas turbines [9]. The CO_2 Brayton cycle operates at pressures above the critical pressure of CO_2 (73.8 bar [10]) for both the high pressure and low pressure side. This is mainly due to these plants being developed for applications where access to low temperature cooling water is very limited. With the low temperature cooling water available at off-shore oil and gas platforms at the NCS it is possible to run the cycle in a transcritical mode, i.e., the pressure after the expansion turbine is below the critical pressure, for better performance and efficiency. The transcritical CO_2 Rankine cycle has also been investigated for applications with low temperature heat sources utilizing the benefit of non-isothermal heat absorbtion due to the supercritical pressure [11]. Walnum et al. [12] studied the off-design performance and possible control strategies of a simple CO_2 Rankine cycle for low temperature applications and compared with a subcritical Organic Rankine cycle.

This paper will evaluate potential CO_2 bottoming cycles and investigate how they behave at reduced gas turbine load. In the following, a description of the modelled processes will be given, the modelling and simulation methods will be described, and the results will be discussed.

2 Models and methodology

To achieve realistic evaluation for the performance of the modelled cycles, detailed component models are necessary. In the following the component models and system solution methods are described.

2.1 Modelled cycles

Compared to steam cycles, the temperature of the CO_2 at the outlet of the expander is much higher. To enable high efficiency systems this heat must be recovered. This is normally done with internal recuperation between the low pressure flow from the expander and the high pressure flow from the pump, see Figure 1, left. This drastically reduces the exergy losses in the condenser compared to a non-recuperated cycle, but as the temperature at the inlet of the waste heat recovery unit (WHRU) increases, the potential heat recovery is also reduced. Lately several companies have investigated the potential for utilising the high expander outlet temperature in a dual stage system. Lehar [13] describes a dual stage layout including an advanced condensation system to reduce the compressor inlet temperature, and Held et al. [14] describes mulitple configurations for dual stage supercritical CO_2 systems and a mass management system for control of the cycle. An alternative if the platform has a heat demand will be to utilise the rest heat after the expander for this purpose.

Two layouts have been investigated in order to evaluate the potential of CO_2 based bottoming cycles; one single stage cycle and one dual stage cycle, see Figure 1. For operation on the NCS it is assumed that cooling water at 10 °C is available throughout the year. This enables transcritical operation with heat rejection at subcritical pressures, and the cycles are therefore equipped with a low pressure receiver for charge management. This is common in several CO_2 refrigeration applications [15]. Due to the availability of cold sea water, the effect of cooling water temperature is not studied. The available cooling water temperature has a large influence on the power output of the bottoming cycle. The CO_2 cycle is especially sensitive to this as the condensation temperature approaches and even exceeds the critical point (31 °C). In that case the cycle would need to operate as a fully supercritical Brayton cycle. The effect is further shown in [9].

This is the accepted version of an article published in Energy
http://dx.doi.org/10.1016/j.energy.2013.06.071

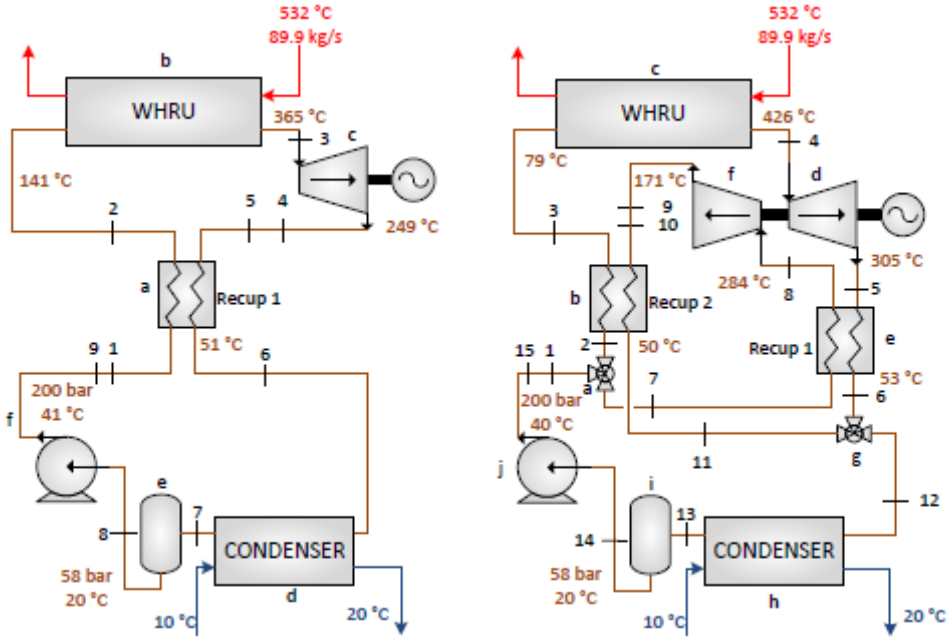

Figure 1: Process flow diagram of single and dual stage system. Selected design point stream data are included.

2.2 Definitions

The gas turbine gross electrical power output is defined as:

$$\dot{W}_{gt} = \left(\dot{W}_{shaft}\eta_{gen}\right)_{gt}$$

where $\dot{W}_{shaft}$ is the shaft power and η_{gen} is the generator efficiency.

The CO_2 bottoming cycle gross electrical power output is defined as:

$$\dot{W}_{bc} = \left[\sum_{i=1}^{n} \dot{W}_{shaft,exp(i)}\right]\eta_{gen} - \dot{W}_{shaft,pump}/(\eta_{mot}\eta_{VFD})$$

where $\dot{W}_{shaft,exp(i)}$ is the shaft power of expander *i* of *n* expanders in the cycle, $\dot{W}_{shaft,pump}$ is the shaft power of the CO_2 pump and η_{mot} and η_{VFD} is the efficiency of the pump motor and variable frequency drive respectively.

The net plant power output is defined as:

$$\dot{W}_{net,plant} = \dot{W}_{gt} + \dot{W}_{bc} - \dot{W}_{aux}$$

where $\dot{W}_{aux}$ is the auxiliary power requirement.

The net plant efficiency is defined as:

$$\eta_{net,plant} = \frac{\dot{W}_{net,plant}}{(\dot{m}LHV)_{fuel}}$$

This is the accepted version of an article published in Energy
http://dx.doi.org/10.1016/j.energy.2013.06.071

where $\dot{m}_{fuel}$ is the mass flow of fuel and LHV_{fuel} is the lower heating value of the fuel.

2.3 Basis for calculations

Assumptions for the different sub-systems and components, as well as the gas turbine, need to be defined in order to evaluate the CO_2 bottoming cycles in detail.

2.3.1 Gas turbine

The gas turbine performance was calculated separately with GT MASTER from Thermoflow Inc. [16]. The chosen model is a GE LM2500+G4 with the dry low emission (DLE) setup. Compressor and turbine maps relating corrected inlet air mass flow to compressor pressure ratio and efficiency were utilized. Assumptions for the GT are listed in Table 1.

Table 1: Gas Turbine model assumptions

Ambient	
Temperature [°C]	15
Pressure [bar]	1.013
Relative humidity [%]	60
Gas Turbine	
Model type	GE LM2500+G4 DLE
Fuel	Methane
Inlet pressure drop [bar]	0.010

2.3.2 Bottoming cycle design assumptions

The first design of the CO_2 bottoming cycles models were performed in Aspen HYSYS [17], to enable simple modifications and tuning of the processes. However, since HYSYS does not use real heat exchanger performance parameters for heat transfer coefficients and pressure drop, more detailed models are needed to achieve realistic results, especially at off-design conditions. An in-house model was therefore used for the detailed simulations. The HYSYS models were used to validate the results from the in-house simulation tool at design condition. The design point parameters shown in Table2 were used to define the HYSYS model and the heat exchanger models in the in-house tool was designed to yield the same input and output states as in HYSYS. All the parameters stated in Table 2 are valid only for operation at design point conditions. For example, the UA values for the heat exchangers will vary according to the heat transfer coefficients found with the chosen heat transfer correlations used, as shown in Table 3. In this way, a close approximation to real off-design results may be achieved.

This is the accepted version of an article published in Energy
http://dx.doi.org/10.1016/j.energy.2013.06.071

Table 2: Bottoming cycle process and component design point parameters

Parameter	Value
WHRU UA [kW/K]	400
Recuperator 1 UA [kW/K]	1000
Recuperator 2 UA [kW/K]	250
Max pump outlet pressure [bar]	200
Condensation temperature [°C]	20
Cooling water temperature [°C]	10
Cooling water temperature increase [K]	10
Pump efficiency [%]	80
Expander efficiency [%]	85
Motor/generator efficiency [%]	95

In the following, the unit models and how they are coupled together will be described.

2.3.3 Heat exchangers

An in-house framework is used to model the heat exchangers. The models use geometrical input data to calculate parameters such as hydraulic diameters, perimeters and cross sectional areas for each fluid pass. Based on the geometry specification and the fluid inlet conditions, the outlet conditions are found through integration of the fluid passes (with a 4th order Runge Kutta routine) and iteration on the wall temperature profile (with DNSQE from SLATEC [18]). Relevant heat transfer and pressure drop correlations from literature are utilized, see Table 3. More details on the heat exchanger framework can be found in [19].

Table 3: Heat transfer and pressure drop correlations

WHRU	Correlation
Fin side heat transfer	Næss [20]
Fin side pressure drop	Næss [20]
Tube side heat transfer	Gnielinski [21]
Tube side pressure drop	Selander [22]
Condenser	
Single phase heat transfer	Martin [23]
Condensing heat transfer	Han Lee Kim [24]
Single phase pressure drop	Martin [23]
Condensing pressure drop	Han Lee Kim [24]
Recuperators	
Single phase heat transfer	Gnielinski [21]
Single phase pressure drop	Selander [22]

Waste heat recovery unit (WHRU)

The WHRU is modelled as a crossflow finned tube heat exchanger with serrated fins. The tube passes are arranged in horizontal serpentines inside a rectangular vertical gas duct, approaching a counterflow configuration. The WHRU is designed for a 3 kPa pressure drop on the exhaust side.

Condenser

The condenser is modelled as a plate heat exchanger. The high condensing pressure of CO_2 (55–60 bar) makes it unsuitable for standard plate-and-frame configurations; however plate-and-shell configurations could be an option. In this work, the performance characteristics of the heat exchanger at off-design conditions is of most interest, and this will be relatively independent of the type of heat exchanger.

This is the accepted version of an article published in Energy
http://dx.doi.org/10.1016/j.energy.2013.06.071

The condenser is assumed to be cooled with sea water at 10 °C. At the design point, the cooling water flow rate is set to give 10 °C increase in cooling water temperature, and this flow rate is kept constant also at off-design conditions.

Recuperators

The recuperator model is based on stacked layers of multi-port tubes with counter-current flow, and is meant to represent a generic compact heat exchanger. Due to the high operation pressure (200 bar), diffusion bonded printed circuit heat exchanger might be the most relevant solution currently available.

Table 4: Heat exchanger input parameters

WHRU	Recuperator	Condenser
Duct width[a]	Length	Length
Duct height[b]	Number of layers	Width
Duct depth[c]	Number of channels	Number of channels
Tube wall thickness	Channel diameter	Channel distance
Tube inner diameter	Wall thickness	Chevron angle
Fin height		Surface enhancement factor
Fin thickness		
Fin pitch		
Fin serrated segment height		
Fin serrated segment width		
Number of tubes per row		
Number of parallel rows		
Number of row passes		

[a] Defines tube length

[b] Width x height is exhaust cross section area

[c] Defines exhaust flow length

2.3.4 Pump and turbine

The pump and expanders are modelled with constant isentropic efficiencies defined as follows:

$$\eta_{Pump} = \frac{h(p_{out}, s_{in}) - h_{in}}{h_{out} - h_{in}}, \qquad \eta_{turbine} = \frac{h_{in} - h_{out}}{h_{in} - h(p_{out}, s_{in})}$$

The efficiencies are set to 80 % and 85 % for the pump and turbines respectively through-out the studied load range. The effect of the constant efficiency assumption will be further discussed in section 3.2.2. It is assumed that the pump was equipped with variable frequency drive (VFD) and the turbines with variable inlet guide vanes (VIGV).

2.3.5 System balancing solution

Stationary solutions for the whole bottoming cycle is solved using a sequential quadratic programming (SQP) method (NLPQL [25]). The numbered ticks in Figure 1 show the calculation path for the cycle and represent the state points and are defined by pressure and enthalpy. The state at the inlet of the recuperator (1) is guessed (the pressure is defined and the temperature is guessed). Since the state at the outlet of the expander is necessary for calculating the system, an extra iteration node (number 5 or 10) is included, where the temperature and pressure are guessed. Based on this, all the components can be calculated in the shown calculation sequence (a → f or a → j). For balancing the system when the high pressure and mass flow are set, there are three variables: pump outlet temperature, expander outlet temperature and expander outlet pressure. The variables are constrained so that the following equality constraints are fulfilled: equal enthalpy in node 1 and 9, equal enthalpy in node 4 and 5, and

This is the accepted version of an article published in Energy
http://dx.doi.org/10.1016/j.energy.2013.06.071

saturated liquid outlet from the condenser. The rest of the nodes are calculated through the definition of the components. The NLPQL routine then simultaneously solves the constrained variables and optimizes the pump outlet pressure and mass flow rate. For the dual stage cycle the mass split ratio is an additional optimization variable.

2.3.6 Thermodynamics

CO_2 properties were obtained with the Span-Wagner equation of state [26]. The reference state is chosen according to the International Institute of refrigeration [10]. As the equation is relatively computationally heavy, an tabular version is implemented in the simulation model [27]. The SRK equation of state [28] is used to obtain the properties of exhaust. This is sufficiently accurate as the outlet temperature is well above the water dew point. For water, the IAPWS-97 [29] formulation is utilized. The same equations of states were used in the HYSYS design model.

2.4 Control strategy

For off-design simulation, a control strategy must be chosen for the bottoming cycle. As the cycle is operating in a transcritical mode with a low pressure receiver, the low pressure will be vapour-liquid-equilibrium controlled. This means that the condensation pressure will be controlled by the heat rejected in the condenser, resulting in a saturated liquid outlet from the condenser.

The condensation pressure could to some degree be controlled by the flow of cooling water, but in these simulations it is decided to keep the cooling water flow constant. The mass flow and pump outlet pressure is controlled by the turbine and pump operation. The VFD of the CO_2 pump enables a high efficiency in a wide range of flow rates and pressure ratios. The VIGV allows the turbine to operate with constant pressure ratios over a broad flow range [30]. Based on this, the mass flow rate and high pressure are considered free variables and are optimised during simulation. For the dual stage cycle there is an additional control variable, the flow distribution between the two stages, but there is also an additional control option, with the guide vanes of the additional expander.

The compressor of the LM2500+G4 GT has variable guide vanes in order to increase part load efficiency [31]. This again affects the combined cycle performance at part load conditions. In addition, the DLE setup has fuel staging, where for each stage the flame temperature will range between its maximum value for allowable NO_x emissions and its minimum for allowable CO emissions or flame blowout. Because of this, the turbine exhaust temperature will vary up or down with decreasing load, as shown in Figure 5.

3 Results and discussion

Characteristic for two different CO_2 bottoming cycles has been calculated based on the assumption given in Section 2 at both design and off-design conditions.

3.1 Design point results

Table 5 shows the results from the design point calculations of the simple cycle gas turbine and the two combined cycles, utilizing CO_2 bottoming cycles.

This is the accepted version of an article published in Energy
http://dx.doi.org/10.1016/j.energy.2013.06.071

Table 5: Results from calculations at design point (100 % GT load)

Plant type	Simple cycle	Combined cycle single stage	Combined cycle dual stage
Gas Turbine	GE LM2500+G4	GE LM2500+G4	GE LM2500+G4
Bottoming cycle	None	Single stage CO_2	Two stage CO_2
Net plant power output [MWe]	32.2	41.1	42.0
GT gross power output [MWe]	32.5	32.1	32.1
CO_2 BC gross power output [MWe]	-	9.5	10.4
Net plant efficiency [%]	38.3	48.9	50.0
Exhaust mass flow [kg/s]	89.9	89.9	89.9
Exhaust Temperature after WHRU [°C]	528	170	126

The performance of the CO_2 bottoming cycles matched well with the HYSYS models. However the performance drop due to inclusion of pressure drop was about 0.5 MW for both cycles. This shows the importance of including such irreversibilities. The results presented in Table 5 include pressure drops as well as real heat exchanger performance.

An interesting point to note is the relatively small difference in power output between the single stage and the dual stage process. This shows that relatively high efficiencies can be reached in single-stage cycles if using a high degree of recuperation.

The temperature – enthalpy diagram for the two bottoming cycles, as well as temperature curves for the heat source and sink, are shown in Figure 2. The properties at the state points are shown in Table 6. Compared to subcritical cycles, which mainly operates within and around the two-phase area, one can see that the CO_2 cycles mostly operates far above the critical point and only barely enters the two-phase area in the condenser.

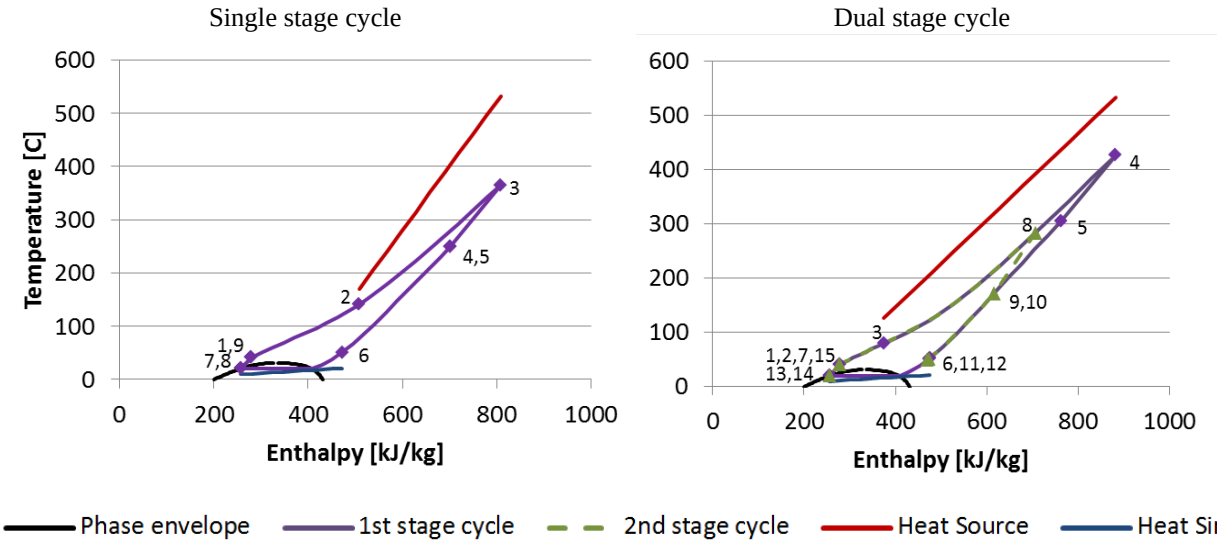

Figure 2: Temperature – enthalpy diagram for the two bottoming cycles.

This is the accepted version of an article published in Energy
http://dx.doi.org/10.1016/j.energy.2013.06.071

Table 6: Thermodynamic properties at defined state points

Single Stage

State point	Pressure [bar]	Enthalpy [kJ/kg]	Temperature [C]	Density [kg/m^3]	Mass flow [kg/s]
1	200.0	279.8	41.2	833.3	121.2
2	199.9	508.6	141.3	344.6	121.2
3	195.5	808.6	365.2	163.1	121.2
4	58.7	701.6	249.4	61.5	121.2
5	58.7	701.6	249.4	61.5	121.2
6	58.3	472.7	51.3	128.4	121.2
7	58.1	257.9	20.6	767.0	121.2
8	58.1	257.9	20.6	767.0	121.2
9	200.0	279.8	41.2	833.3	121.2
Exhaust inlet	1.0432	920.7	532.0	0.43	89.9
Exhaust outlet	1.0132	516.2	170.0	0.78	89.9

Dual Stage

State point	Pressure [bar]	Enthalpy [kJ/kg]	Temperature [C]	Density [kg/m^3]	Mass flow [kg/s]
1	200.0	277.9	40.4	837.8	130.9
2	200.0	277.9	40.4	837.8	78.5
3	200.0	374.5	79.4	598.0	78.5
4	197.2	882.9	426.1	147.4	78.5
5	59.2	762.9	304.8	55.1	78.5
6	57.7	476.7	53.4	124.3	78.5
7	200.0	277.9	40.4	837.8	52.3
8	199.8	707.1	283.7	199.6	52.3
9	57.8	616.1	171.2	73.8	52.3
10	57.8	616.1	171.2	73.8	52.3
11	57.7	471.2	49.7	128.1	52.3
12	57.7	474.5	51.9	125.8	130.9
13	57.3	256.0	20.0	773.0	130.9
14	57.3	256.0	20.0	773.0	130.9
15	200.0	277.9	40.4	837.8	130.9
Exhaust inlet	1.0432	920.7	532.0	0.43	89.9
Exhaust outlet	1.0132	477.1	125.6	0.86	89.9

From Figure 2 it can be observed that the single stage process is approaching a limit for how much heat can be extracted from the heat source and thereby converted to power, due to the small temperature difference in the low temperature part of the heat exchanger. This indicates that the difference in power output between the two cycles will increase with increasing size of the WHRU. This was further investigated with the HYSYS model and the results are shown in Figure 3. As seen, the increase in power output with increase in WHRU size for the dual stage cycle is higher than for the single stage cycle.

This is the accepted version of an article published in Energy
http://dx.doi.org/10.1016/j.energy.2013.06.071

A CO_2 bottoming cycle plant will have several heat exchangers that make up a large part of the total system weight. Therefore there exist a potential for optimizing the distribution of weight between the heat exchangers, to find the highest possible power-to-weight ratio.

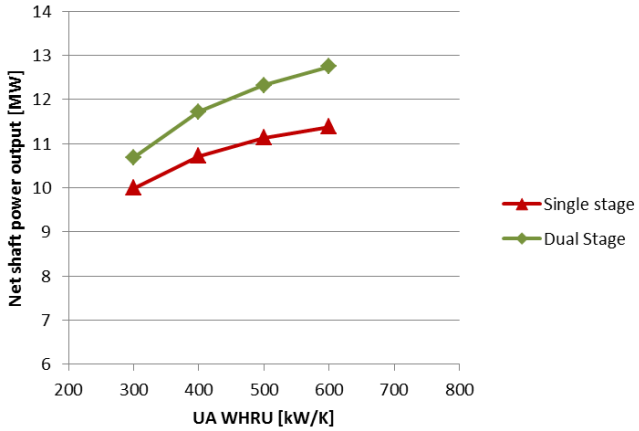

Figure 3: Bottoming cycle shaft power output from HYSYS vs WHRU size

Compared to the simple cycle GT, a CO_2 bottoming cycle will increase the power output with about 30 %, which is similar to that claimed in [9]. According to results presented by Nord et al. [4], a once through steam bottoming cycle could yield a power output of 11.3 MW with the same gas turbine as used in this work. The power output found for CO_2 with the current assumptions is 8 and 16 % lower for the dual- and single stage cycles respectively. The main benefit of the CO_2 cycle is that the high mean pressure level, that makes the equipment very compact [9]. The mass flow rate of CO_2 is about 10 times that of a similar steam cycle, but the density is about 20 times higher at the turbine inlet and 1500 times higher at the turbine outlet.

Also, since the pressure in the CO_2 cycle always is higher than the ambient pressure, there is no need for a treatment plant. In a steam system, a water treatment plant is necessary. There will however always be some leakages from a system, so a make-up tank and periodically refilling of CO_2 will be required. The make-up tank will normally also function as the receiver and be a part of the charge management control.

As for all Rankine cycles the efficiency of the turbomachinery is highly influential on the power output. Due to the high power density, design of CO_2 turbomachinery has some different challenges compared to conventional turbomachinery [32].

One important difference between CO_2 and steam cycles is that the pump power is much higher relatively to the expansion power. For the single stage cycle, the pump power is about 2.7 MW and the expander power is about 13.0 MW while for the dual stage cycle it is 2.9 MW and 14.2 MW (total for both expanders) respectively, meaning that about 20% of the expansion work is used for pumping. This is because the pumping takes place close to the critical point and the fluid is thus not incompressible as is the assumption for a liquid.

Due to the relatively recent development of the CO_2 cycles, the available performance data on turbomachinery is very limited, especially at the MW scale. As a consequence the efficiencies assumed in this work are based on more conventional equipment. Figure 4 shows the sensitivity of the turbomachinery isentropic efficiency on the system net gross power in the design point for the single stage cycle. It is assumed that the rest of the cycle is unaffected. One can see that the relationship is approximately linear for both the pump and expander. A 5 % increase in the expander efficiency will yield a 5 % higher power output and thereby a 6.3 % increase in net output. A 5 % increase of the pump efficiency will yield a 5 % reduction in pump work, and thereby a 1.3 % increase in net shaft output. This is not completely accurate as a change in efficiency will also have an impact on the outlet

This is the accepted version of an article published in Energy
http://dx.doi.org/10.1016/j.energy.2013.06.071

temperature and thereby influence the rest of the cycle, but the differences should be relatively small. As might be expected, the efficiency of the turbine is much more important than for the pump. This was also shown by Sakar in [33] for supercritical CO_2 recompression Brayton cycles.

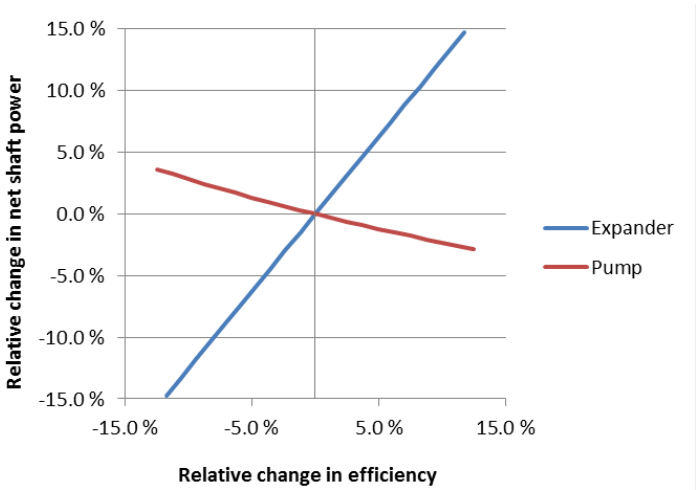

Figure 4: Sensitivity of turbomachinery efficiencies

3.2 Off-design results

3.2.1 Gas turbine results

Off-design parameters for the gas turbine that are used as input to the off-design calculations of the CO_2 bottoming cycles are shown in Figure 5. The exhaust mass flow rate is almost proportional to the gas turbine load, while the exhaust temperature is reduced down to 90 % load and then increases as the load is further reduced. This is an effect of the DLE system as described in Section 2.4.

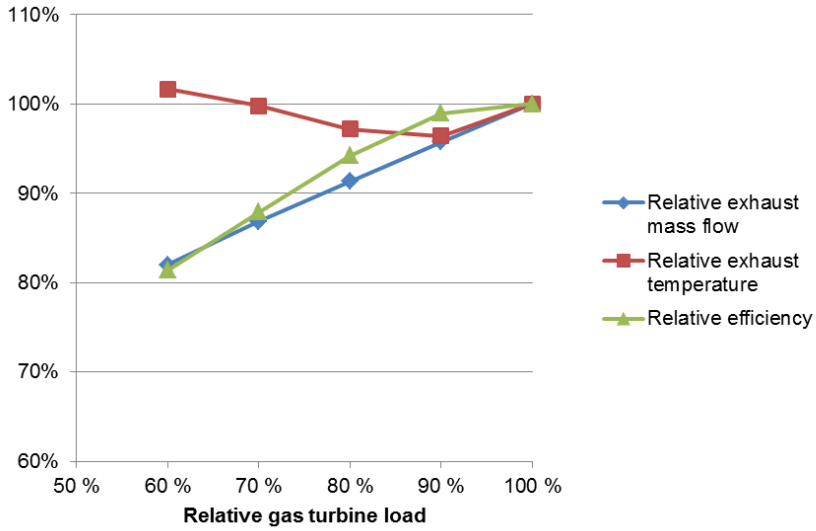

Figure 5: Relative GT efficiency, exhaust mass flow and temperature vs gas turbine load

3.2.2 Bottoming cycle results

The off-design results for the CO_2 bottoming cycles are shown in Figure 6. BC denotes results for only the bottoming cycle and CC denotes the combined cycle (GT plus BC). We can see that the relative changes in output from the two cycles are approximately equal. The dual stage cycle drops slightly more off for the 90 % load case. This is where the exhaust temperature from the gas turbine is at its

This is the accepted version of an article published in Energy
http://dx.doi.org/10.1016/j.energy.2013.06.071

lowest, and this indicates as expected that the gain of utilizing a two stage cycle increases with increasing source temperature.

For both cycles one can see how the increase in exhaust gas temperature outweighs the reduction in exhaust mass flow rate at lower gas turbine loads. This is also shown by the exergy content of the gas turbine exhaust. As the gas turbine load is reduced, the efficiency of the gas turbine is reduced. The exergy content in the exhaust is however reduced only slightly for GT loads lower than 90%, as more of the energy input from the fuel is left in the gas. One can also observe that the exergy efficiency of the bottoming cycle increases with reduced GT load, since the reduction in power output is smaller than the reduction of the exergy content in the exhaust. This is mainly due to less heat being transferred in the heat exchangers, meaning lower temperature differences and thus smaller losses. Reduced flow rates also results in reduced pressure drops. This contributes to high overall plant efficiency even at low GT loads. At 60 % GT load the plant efficiency is 45 % for the dual stage system, compared to 31 % for the gas turbine. The relative change in efficiency for the dual stage cycle is approximately equal to that shown for steam in [5].

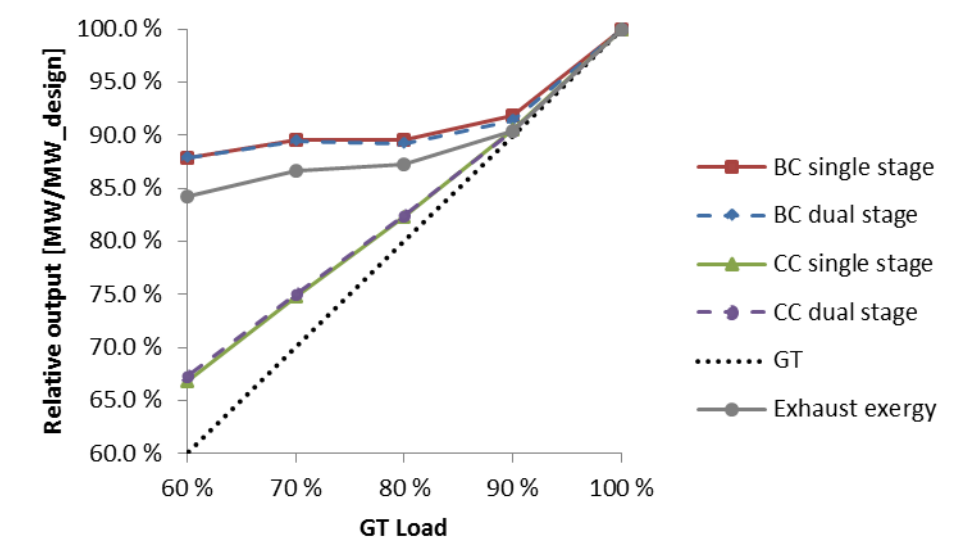

Figure 6: Relative changes in power output vs gas turbine load for the CO_2 bottoming cycles (BC), the full combined cycle plant (CC) and the gas turbine (GT), as well as the relative change in exhaust exergy content.

Performance of the heat exchangers

A major part of the energy conversion in a power cycle takes place in the heat exchangers. Their performance at off-design conditions plays an important role in the total system performance. Figure 7 shows the temperature vs heat transferred in the WHRU and Condenser for the 100 % and 60 % GT load cases for the single stage CO_2 bottoming cycle. Red lines indicate GT exhaust flow, purple indicate working fluid and blue indicate cooling water. An interesting point is that even though the heat duty of the heat exchangers are reduced with reduced flow rates at lower GT loads, the overall temperature differences are not reduced correspondingly, especially for the WHRU. This is due to the reduction in heat transfer coefficients at reduced flow rates. For the condenser, one can see that the condensation pressure is slightly lower for the 60 % case, which will increase the specific power output from the turbine due to increased pressure ratio. However, due to reduced mass flow, this has minimal impact on the overall power output. The reduced condensation pressure is mainly due to reduced average cooling water temperature. As the cooling water flow is kept constant and the condenser duty is reduced the outlet temperature is reduced.

This is the accepted version of an article published in Energy
http://dx.doi.org/10.1016/j.energy.2013.06.071

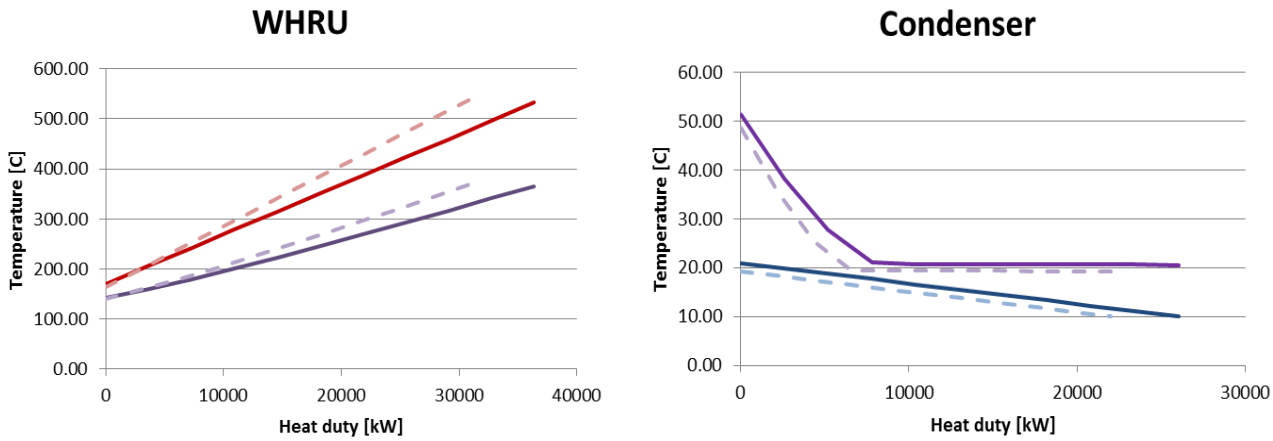

Figure 7: Temperature vs duty curves for the WHRU and Condenser in the single stages system at 100 % (unbroken lines) and 60 % (broken lines).

Variation in rotational equipment conditions

To evaluate the assumption of constant efficiencies for the turbo expander, the variation of volumetric flow rate and velocity ratio (tip speed/spouting velocity) has been calculated. The changes in volumetric flow is about 15 % and the velocity ratio changes from 0.7 (optimum design) to 0.68. Similar characteristics can be found for the expanders in the dual stage cycle. With these relatively small changes, an expander with variable inlet guide vanes should be able to operate with approximately constant efficiency [34]. If the design point for the expander was set to a lower load operating point, the variation from design would be even smaller.

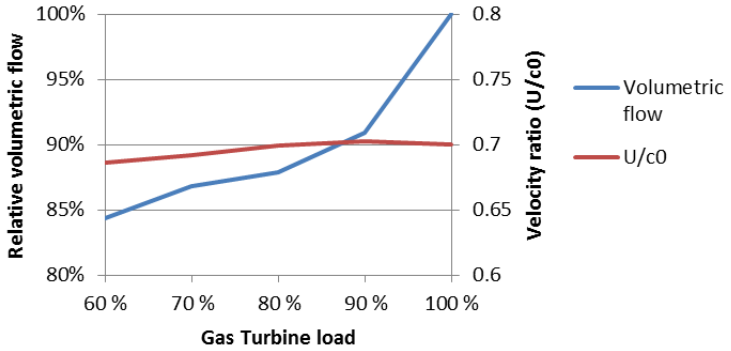

Figure 8: Variation in expander operating conditions for the single stage cycle

The pump operates with approximately constant inlet conditions. The mass flow rate varies with about 18 % between the 100 and 60% gas turbine load cases, pressure ratio being approximately constant. With these variations one would expect a relatively flat efficiency curve, and with a variable frequency drive, the constant efficiency assumption should be acceptable.

4 Conclusions

Inclusion of bottoming cycles to gas turbines on offshore oil and gas installations could be an attractive solution for improved energy efficiency and reduced emissions. The results in this paper show that utilisation of CO_2 as working fluid in the bottoming cycles could be a viable alternative to steam.

This is the accepted version of an article published in Energy
http://dx.doi.org/10.1016/j.energy.2013.06.071

The results show 8 and 16 % lower power output respectively for a dual- and single stage CO_2 cycle compared to compact steam bottoming cycles reported in literature. Taking into account the probable positive characteristics with respect to volume, weight, cost, which are important advantages especially for off-shore applications, the results are highly interesting. It is further shown that the output can be increased if the heat exchanger sizes are increased or the efficiency of the turbomachinery is improved. However, only a techno-economical optimisation may show if this is desirable.

A further aspect is the advantageous off-design characteristics with the proposed control strategy. Gas turbine part load condition of 60% still maintains about 85% net power output from the CO_2 bottoming cycle, resulting in 67 % net plant output. Also the efficiency is kept higher at lower load, with 45 % net plant efficiency at 60 % GT load, compared to 31 % for only the gas turbine. This is especially important for an offshore application, where design conditions are met only for a shorter period of the lifetime of the platform.

The CO_2 bottoming cycle technology is not fully commercially available yet, and compared to steam cycles much less mature. Important development is however on-going and the technology is already demonstrated at scale, and full scale pilots are planned. This will give important information in verifying the results achieved through modelling and simulation.

5 Acknowledgement

This publication forms a part of the EFFORT project, performed under the strategic Norwegian research program PETROMAKS (203310/S60). The authors acknowledge the partners Statoil, TOTAL E&P Norway, Shell Technology Norway, PETROBRAS, and the Research Council of Norway for their support.

References

[1] Vanner R. Energy Use in Offshore Oil and Gas Production: Trends and Drivers from 1975 to 2025. London, United Kingdom: Policy Studies Institute (PSI); 2005.

[2] Nguyen T-V, et al., Exergetic assessment of energy systems on North Sea oil and gas platforms, Energy (2013), http://dx.doi.org/10.1016/j.energy.2013.03.011

[3] Kloster P. Energy Optimization on Offshore Installations with Emphasis on Offshore Combined Cycle Plants. Conference Energy Optimization on Offshore Installations with Emphasis on Offshore Combined Cycle Plants, Aberdeen, UK; 1999.

[4] Nord LO, Bolland O. Steam bottoming cycles offshore – Challenges and possibilities. Journal of Power Technologies. 2012;92(3):201–7.

[5] Nord LO, Bolland O. Design and off-design simulations of combined cycles for offshore oil and gas installations. Applied Thermal Engineering. 2013;54(1):85-91.

[6] Johnson GA, McDowell MW, O'Connor GM, Sonwane CG, Subbaraman G. Supercritical CO2 cycle development at Pratt & Whitney Rocketdyne. ASME Turbo Expo. Copenhagen, Denmark: ASME; 2012.

[7] Kimball KJ, Clementoni EM. Supercritical carbon dioxide brayton power cycle development overview. ASME Turbo Expo. Copenhagen, Denmark: ASME; 2012.

[8] Wright SA, Conboy TM, Rochau GE. Supercritical CO2 power cycle development summery at Sandia National Laboratories. International Conference on ORC Power Systems. Delft 2011.

[9] Persichilli M, Kacludis A, Zdankiewicz E, Held T. Supercritical CO2 Power Cycles Developments and Commercialization: Why sCO2 can Displace Steam. Power-Gen India & Central Asia. New Delhi, India 2012.

[10] Lemmon EW, Huber LM, McLinden MO. Refrence Fluid Thermodynamic and Transport Properties (REFPROP). NIST Standard Refrence Database 23 Version 8 2007.

[11] Vélez F, Segovia J, Chejne F, Antolín G, Quijano A, Carmen Martín M. Low temperature heat source for power generation: Exhaustive analysis of a carbon dioxide transcritical power cycle. Energy. 2011;36(9):5497-507.
[12] Walnum HT, Rohde D, Ladam Y. Off-design analysis of ORC and CO2 power production cycles for low-temperature surplus heat recovery. International Journal of Low-Carbon Technologies. 2013;8(1):29-36.
[13] Lehar MA. Dual reheat rankine cycle system and method thereof, European Patent EP 2 345 793 A2 2010
[14] Held TJ, Vermeersch ML, Xie T, Miller JD. Heat engines with cascading cycles, Pending World Patent WO/2011/119650. 2011.
[15] Nekså P, Walnum HT, Hafner A. Keynote: CO2 - a refrigerant from the past with prospects of being one of the main refrigerants in the future. Conference Keynote: CO2 - a refrigerant from the past with prospects of being one of the main refrigerants in the future, Sydney, Australia. International Institute of Refrigeration, IIR/IIF.
[16] Thermoflow. GT MASTER 21.0. 2011.
[17] Aspen Technology Inc. Aspen HYSYS v7.2. 2010.
[18] SLATEC - Common Mathematical Library. Computer Science Dept UT, Laboratory ORN, Netlib Repository. Version 4.1 1993. Available at: http://www.netlib.org/slatec/
[19] Skaugen G, Kolsaker K, Walnum HT, Wilhelmsen Ø. A Flexible and Robust Modelling Framework for Multi-Stream Heat Exchangers. Computers & Chemical Engineering. *2013*;49:95-104.
[20] Næss E. An Experimental Study of Heat Transfer and Pressure Drop in Serrated-Fin Tube Bundles and Investigation of Particulate Fouling in Waste Heat Recovery Heat Exchangers. Trondheim, Norway: NTNU, 2007.
[21] Gnielinski V. New Equations for Heat and Mass Transfer in Turbulent Pipe and Channel Flow. International chemical engineering, Vol.16, No. 2, pp. 359-368, 1976.
[22] Selander WN. Explicit Formulas for the Computation of Friction Factors in Turbulent Pipe Flow. Volume 6354 of Atomic Energy of Canada Limited AECL, Chalk River, Ontario CANADA: Chalk River Nuclear Laboratories; 1978.
[23] Martin H. A theoretical approach to predict the performance of chevron-type plate heat exchangers. Chemical Engineering and Processing. 1996;35(4):301-10.
[24] Han D-H, Lee K-J, Kim Y-H. The Characteristics of Condensation in Brazed Plate Heat Exchangers with Different Chevron Angles. J Korean PhysSoc. 2003;43(1):66-73.
[25] Schittkowski K. NLPQL: A fortran subroutine solving constrained nonlinear programming problems. Annals of Operations Research. 1986;5(1):485-500.
[26] Span R, Wagner WU. A new equation of state for carbon dioxide covering the fluid region from the triple-point temperature to 1100 K at pressures up to 800 MPa. J Phys Chem Ref Data. 1996;25(6):1509-96.
[27] Andresen T, Skaugen G. Lookup tables based on Gibbs free energy for quick and accurate calculation of thermodynamic properties for CO2. 22nd International Congress of Refrigeration : Refrigeration creates the future, Beijing, China International Institute of Refrigeration; 2007.
[28] Soave G. Equilibrium constants from a modified Redlich-Kwong equation of state. Chemical Engineering Science. 1972;27(6):1197-203.
[29] Wagner ea. The IAPWS Industrial Formulation 1997 for the Thermodynamic Properties of Water and Steam. ASME J Eng Gas Turbines and Power. 2000;122:150-82.
[30] Meitner PL, Glassman AJ. Off-Design Performance Loss Model for Radial Turbines With Pivoting, Variable-Area Stators. In: NASA, editor. Technical Paper 1708. Cleveland, Ohio1980.
[31] Haglind F. Variable geometry gas turbines for improving the part-load performance of marine combined cycles – Gas turbine performance. Energy. 2010;35(2):562-70.
[32] Fuller R, Noall J, Preuss J. Turbomachinery for supercritical CO2 power cycles. ASME Turbo Expo. Copenhagen, Denmark: ASME; 2012.
[33] Sarkar J. Second law analysis of supercritical CO2 recompression Brayton cycle. Energy. 2009;34(9):1172-8.

This is the accepted version of an article published in Energy
http://dx.doi.org/10.1016/j.energy.2013.06.071

[34] Atlas Copco. Driving Expander Technology. Atlas Copco Gas and Process Solutions. Cologne, Germany, 2012(B03/004/24/0512).

This is the accepted version of an article published in Energy
http://dx.doi.org/10.1016/j.energy.2013.06.071